Suzaku Observations of ULIRGs

Andrew Ptak (JHU / GSFC)

In collaboration with:
V. Braito (Leicester U.), J. Reeves (Keele), T. Yaqoob (JHU / GSFC)

R. Fujimoto (Kanazawa U.) and Arp 220 SWG Team

Overview

- Ultraluminous Infrared Galaxies (ULIRGs) are defined to be galaxies with $L_{FIR} > 10^{12}\ L_{sun}$
- Most/all are merger systems – drives gas towards nucleus
- Important phase of galaxy evolution (Hopkins et al. 2007, 2008) – may be precursors to quasar phase
- Energy budget between AGN and star formation is uncertain
  - SFR > 100 solar masses yr^{-1} if mostly star formation

Hopkins et al. (2008)

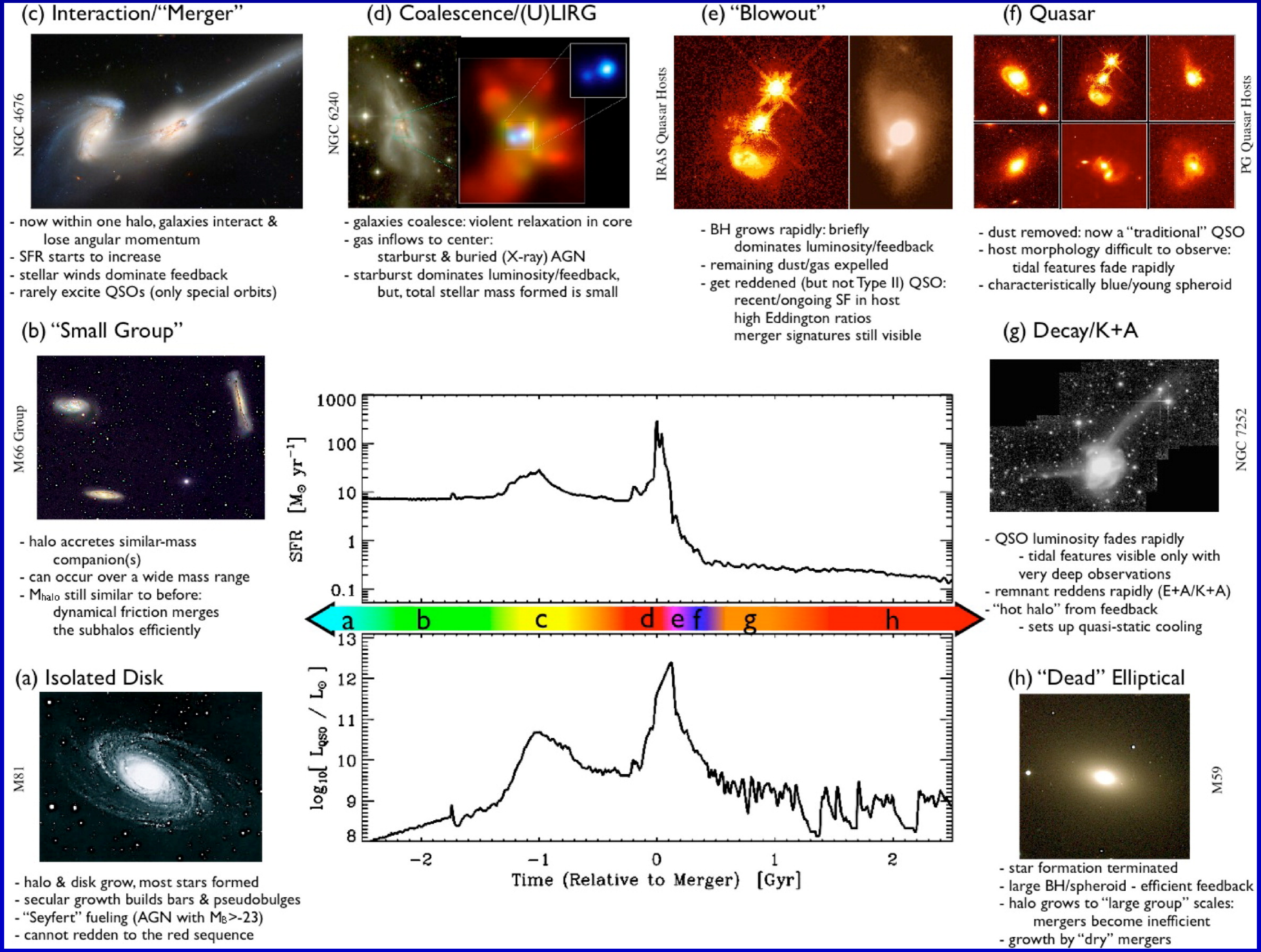

Source	α_6	τ	α_{bol}	O/X/L	Source	α_6	τ	α_{bol}	O/X/L
ARP 220	75±1	1.40±0.01	$9.8^{+3.7}_{-2.7}$	L[1]/SB[4]/SB[10]	IRAS 14197+0813	75±2	2.10±0.14	10^{+5}_{-4}	–/–/–
IRAS 00091−0738†	90±1	1.81±0.04	25^{+8}_{-7}	SB[1]/–/–	IRAS 14252−1550	< 20	< 0.04	< 0.9	L[1]/–/SB[10]
IRAS 00188−0856	96±1	0.60±0.02	45±9	L[1]/–/A*[10]	IRAS 14348−1447	51^{+3}_{-5}	< 0.09	$3.7^{+2.1}_{-1.5}$	L[1]/–/SB[11]
IRAS 00456−2904	< 1.0	0	< 0.04	SB[1]/–/–	IRAS 15130−1958	91^{+1}_{-3}	< 0.01	28^{+9}_{-11}	A[1]/–/A[10]
IRAS 00482−2721	< 54	< 0.04	< 4.1	L[1]/–/–	IRAS 15206+3342	52±1	0.30±0.02	$3.9^{+1.7}_{-1.2}$	SB[1]/–/SB[10]
IRAS 01003−2238†	96±1	1.58±0.02	49±9	SB[1]/–/–	IRAS 15225+2350	89±1	0.77±0.02	22^{+7}_{-6}	SB[1]/–/SB[10]
IRAS 01166−0844	87±1	1.19±0.06	20^{+7}_{-6}	SB[1]/–/–	IRAS 15250+3609	94±1	0.91±0.01	35^{+9}_{-8}	L[2]/SB[6]/–
IRAS 01298−0744†	98±1	1.79±0.02	74^{+8}_{-9}	SB[1]/–/–	IRAS 15462−0450	90^{+1}_{-16}	< 0.01	25^{+10}_{-18}	A[1]/–/–
IRAS 01569−2939	85±1	1.13±0.04	17^{+6}_{-5}	SB[1]/–/–	IRAS 16090−0139	89±1	0.69±0.01	23^{+7}_{-6}	L[1]/–/A*[10]
IRAS 02411+0353	< 17	< 0.01	< 0.8	SB[1]/–/–	IRAS 16156+0146	90±1	0.37±0.01	25^{+8}_{-6}	A[1]/–/–
IRAS 03250+1606	< 3.4	< 0.11	< 0.2	L[1]/–/A*[10]	IRAS 16468+5200	85±1	0.77±0.02	18^{+6}_{-5}	L[1]/–/SB[10]
IRAS 04103−2838	56±1	0.08±0.02	$4.5^{+2.0}_{-1.4}$	L[1]/–/–	IRAS 16474+3430	< 4.9	< 0.01	< 0.2	SB[1]/–/A*[10]
IRAS 05189−2524	91^{+1}_{-4}	< 0.01	28^{+8}_{-12}	A[1]/A[5]/A[12]	IRAS 16487+5447	21±1	< 0.04	$1.0^{+0.5}_{-0.4}$	L[1]/–/A*[10]
IRAS 08572+3915	99±1	0.44±0.01	85^{+5}_{-6}	L[1]/–/A[10]	IRAS 17028+5817	< 1.2	0	< 0.05	L[1]/–/A*[10]
IRAS 09039+0503	61±1	0.71±0.04	$5.5^{+2.5}_{-1.7}$	L[1]/–/A*[10]	IRAS 17044+6720	91±1	0.32±0.01	26^{+8}_{-6}	L[1]/–/A[10]
IRAS 09116+0334	< 1.8	< 0.01	< 0.07	L[1]/–/A*[10]	IRAS 17179+5444	84±1	0.31±0.02	16^{+6}_{-4}	A[1]/–/A[10]
IRAS 09539+0857†	91±1	1.85±0.03	27^{+8}_{-7}	L[1]/–/SB[10]	IRAS 17208−0014	< 7.9	< 0.01	< 0.4	L[3]/SB[6]/SB[11]
IRAS 10190+1322	< 0.3	0	< 0.02	SB[1]/–/SB[10]	IRAS 19254−7245	89±1	0.21±0.08	23^{+9}_{-7}	A[3]/A[6]/A[11]
IRAS 10378+1109	73^{+1}_{-9}	< 0.01	$9.0^{+3.7}_{-4.6}$	L[1]/–/A*[10]	IRAS 20100−4156	86±1	0.47±0.02	19^{+6}_{-5}	SB[3]/A[6]/SB[11]
IRAS 10485−1447	60±1	0.16±0.03	$5.3^{+2.4}_{-1.7}$	L[1]/–/A*[10]	IRAS 20414−1651	< 2.2	< 0.07	< 0.09	SB[1]/–/SB[10]
IRAS 10494+4424	< 0.4	0	< 0.02	L[1]/–/A*[10]	IRAS 20551−4250†	90±1	1.19±0.01	25^{+8}_{-6}	L[3]/A[6]/A[12]
IRAS 11095−0238†	94±1	1.22±0.01	35^{+9}_{-8}	L[1]/–/SB[10]	IRAS 21208−0519	< 0.9	0	< 0.04	SB[1]/–/SB[10]
IRAS 11130−2659	84±1	1.15±0.02	16^{+6}_{-5}	L[1]/–/–	IRAS 21219−1757	99^{+1}_{-4}	< 0.01	83^{+13}_{-48}	A[1]/–/A[10]
IRAS 11387+4116	< 0.8	0	< 0.03	SB[1]/–/SB[10]	IRAS 21329−2346	43±2	< 0.07	$2.7^{+1.3}_{-0.9}$	L[1]/–/A*[10]
IRAS 11506+1331	54^{+1}_{-21}	< 0.01	$4.2^{+1.9}_{-2.9}$	SB[1]/–/A*[10]	IRAS 22206−2715	< 9.3	< 0.17	< 0.4	SB[1]/–/–
IRAS 12072−0444†	94±1	1.06±0.01	37^{+9}_{-8}	A[1]/–/A[10]	IRAS 22491−1808	< 1.4	0	< 0.06	SB[1]/SB[6]/–
IRAS 12112+0305	< 22	< 0.02	< 1.0	L[1]/SB[6]/SB[11]	IRAS 23128−5919	48±1	0.36±0.03	$3.4^{+1.5}_{-1.0}$	L[3]/A[6]/A[11]
IRAS 12127−1412	98±1	0.24±0.08	60^{+15}_{-14}	L[1]/–/A[10]	IRAS 23234+0946	30^{+2}_{-3}	< 0.05	$1.6^{+0.8}_{-0.6}$	L[1]/–/SB[10]
IRAS 12359−0725	54^{+2}_{-43}	< 0.01	$4.2^{+2.2}_{-3.9}$	L[1]/–/A*[10]	IRAS 23327+2913	73±1	0.86±0.03	$9.1^{+3.8}_{-2.7}$	L[1]/–/SB[10]
[illegible]	< 0.6	[illegible]	< 0.02	L[1]/–/–	MRK 231	93±1	< 0.12	32^{+8}_{-7}	A[1]/A[6]/A[10]
IRAS 13454−2956	59^{+1}_{-28}	< 0.01	$5.0^{+2.2}_{-3.8}$	A[1]/–/–	MRK 273	67^{+1}_{-4}	< 0.01	$7.0^{+2.8}_{-2.7}$	A[1]/A[7]/A[10]
IRAS 13509+0442	< 0.6	0	< 0.03	SB[1]/–/SB[10]	NGC 6240	65^{+6}_{-8}	0.64±0.24	$6.5^{+4.8}_{-3.1}$	L[2]/A[8]/A[12]
IRAS 13539+2920	< 0.4	0	< 0.02	SB[1]/–/SB[10]	4C +12.50	97±1	0.24±0.02	59^{+10}_{-11}	A[1]/–/–
IRAS 14060+2919	< 0.4	0	< 0.02	SB[1]/–/SB[10]	UGC 5101†	92±1	1.09±0.03	30^{+9}_{-8}	L[2]/A[9]/A[10]

Nardini et al. (2008)

X-ray Observations

- X-ray observations have potential to directly observe nuclear continuum
- In practice, AGN in ULIRGs are likely high obscured (N_H >~ 10^{24} cm^{-2})
  - Difficult to draw conclusions from only E<10 keV data
  - Fe-K line detected in some ULIRGs

Chandra and XMM Results

- 0.3-10 keV band typically dominated by starburst (Franceschini, Braito et al. 03, Ptak et al. 03, Teng et al. 05)
- Hot gas surface brightness and temperatures ~ constant between dwarf starbursts -> starbursts -> ULIRGs (Grimes et al. 2005)

Chandra Images of ULIRGs

Mkn 273
UGC 05101
Arp 220
IRAS23128

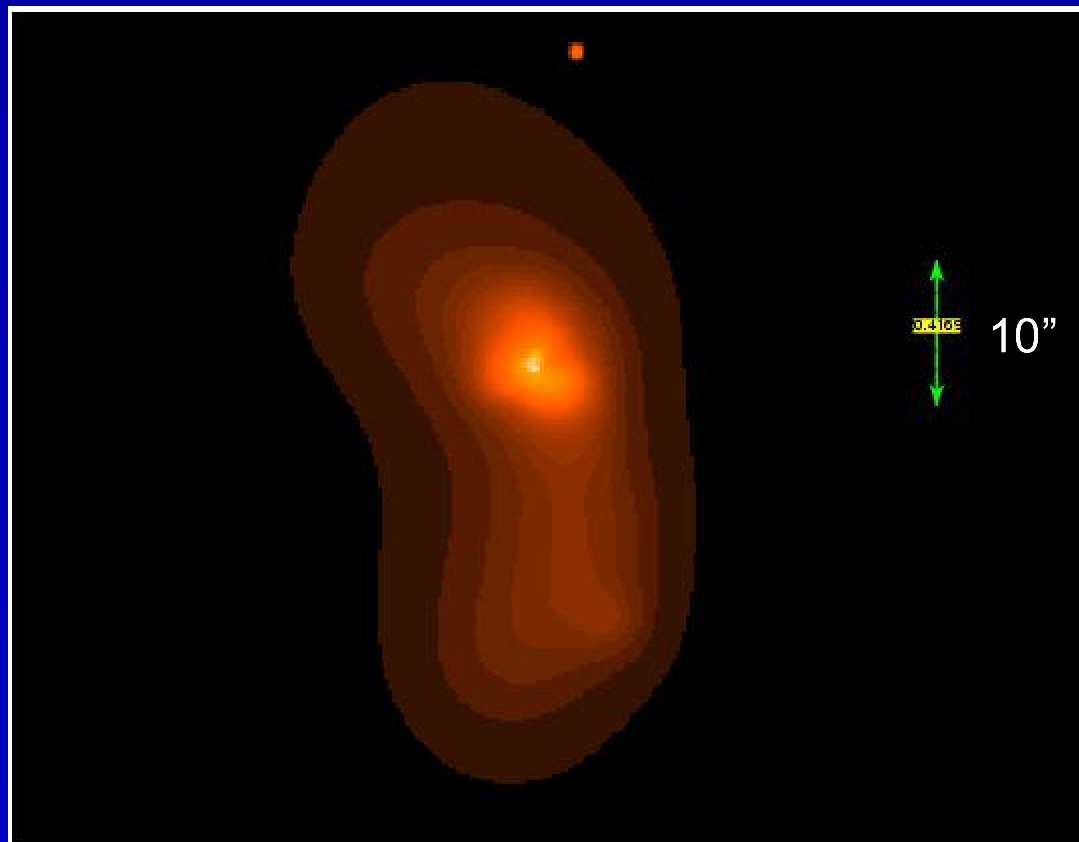

Chandra Images of ULIRGs

Mkn 273
UGC 05101
Arp 220
IRAS23128

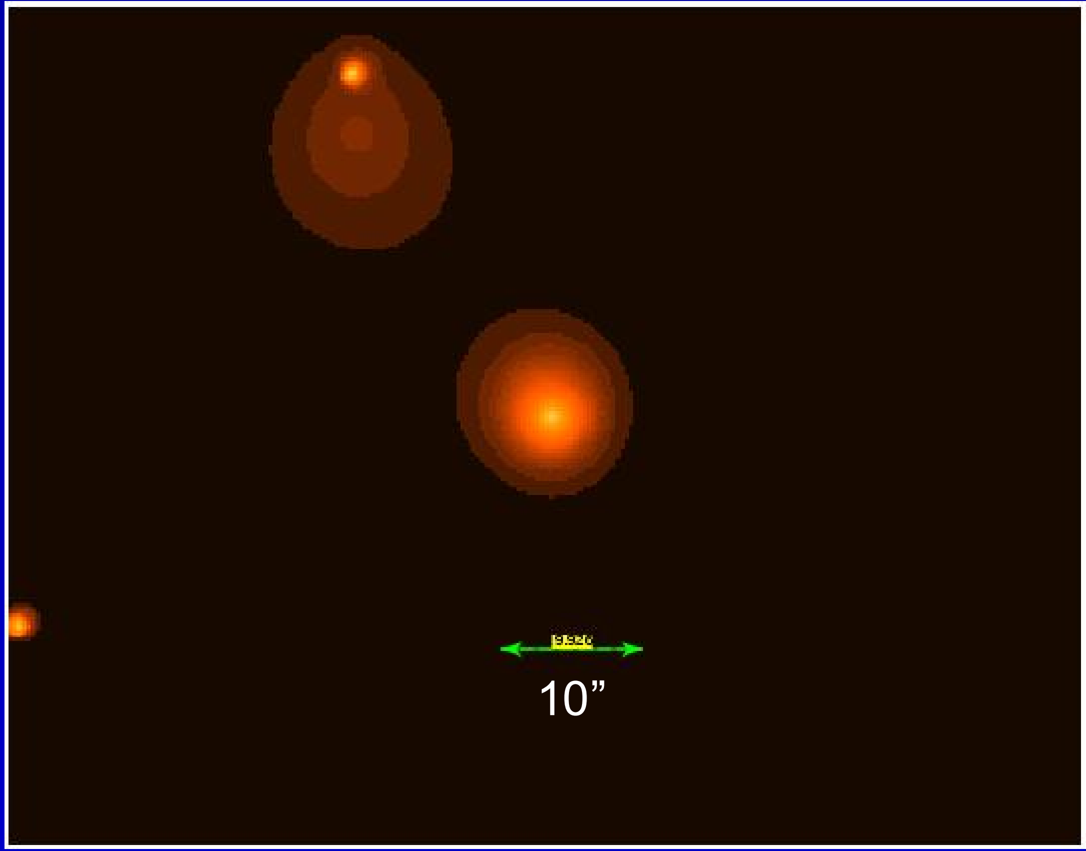

Chandra Images of ULIRGs

Mkn 273
UGC 05101
Arp 220
IRAS23128

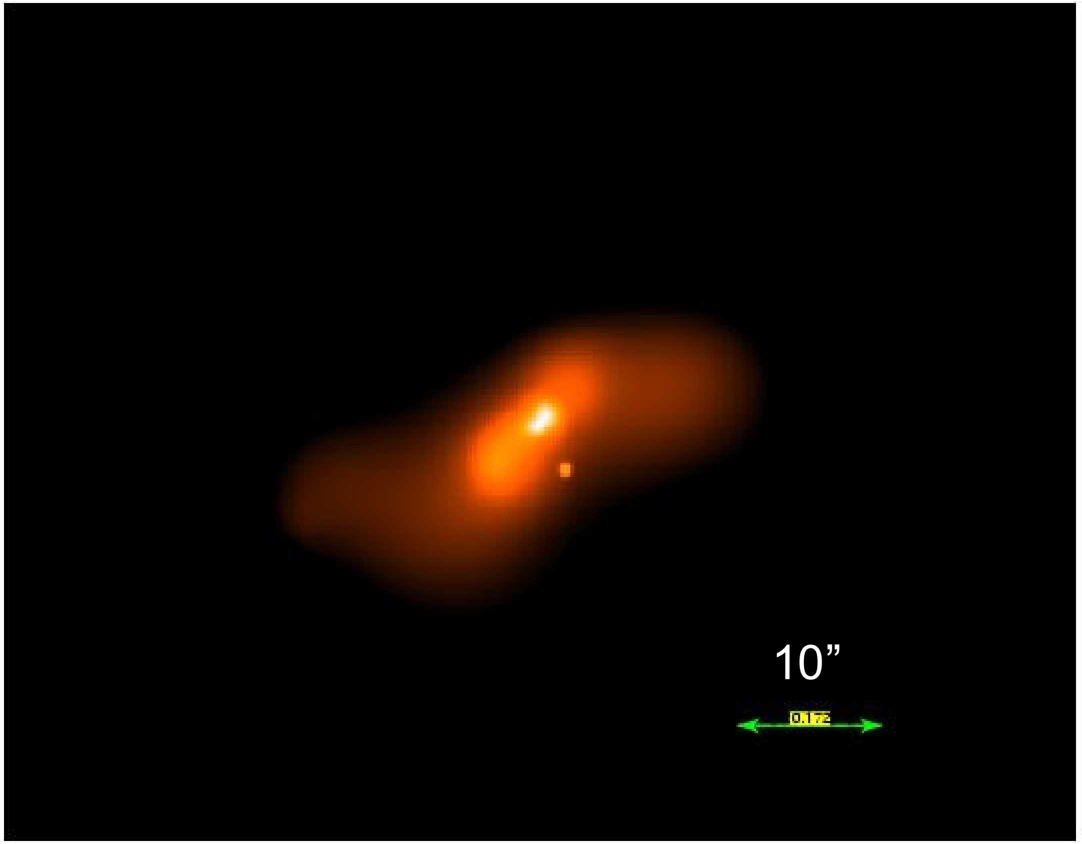

Chandra Images of ULIRGs

Mkn 273
UGC 05101
Arp 220
IRAS23128

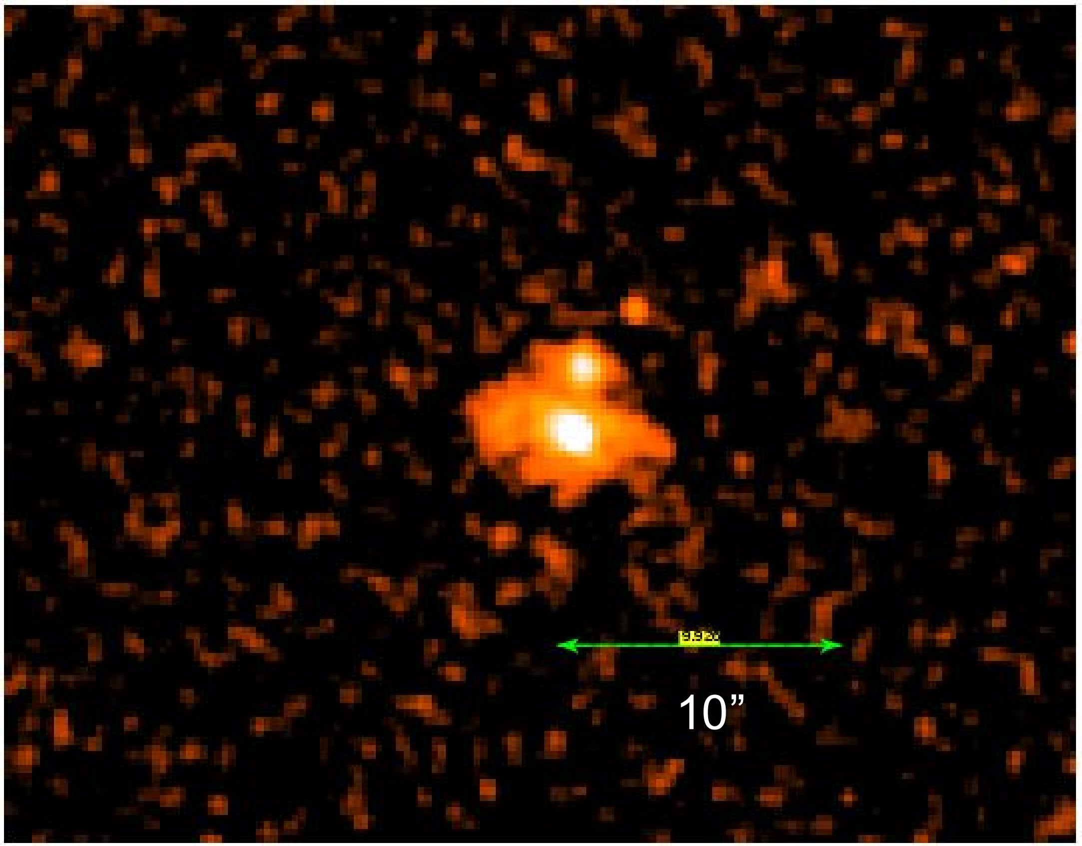

XMM Observation of Arp 220 (Iwasawa et al. 2005)

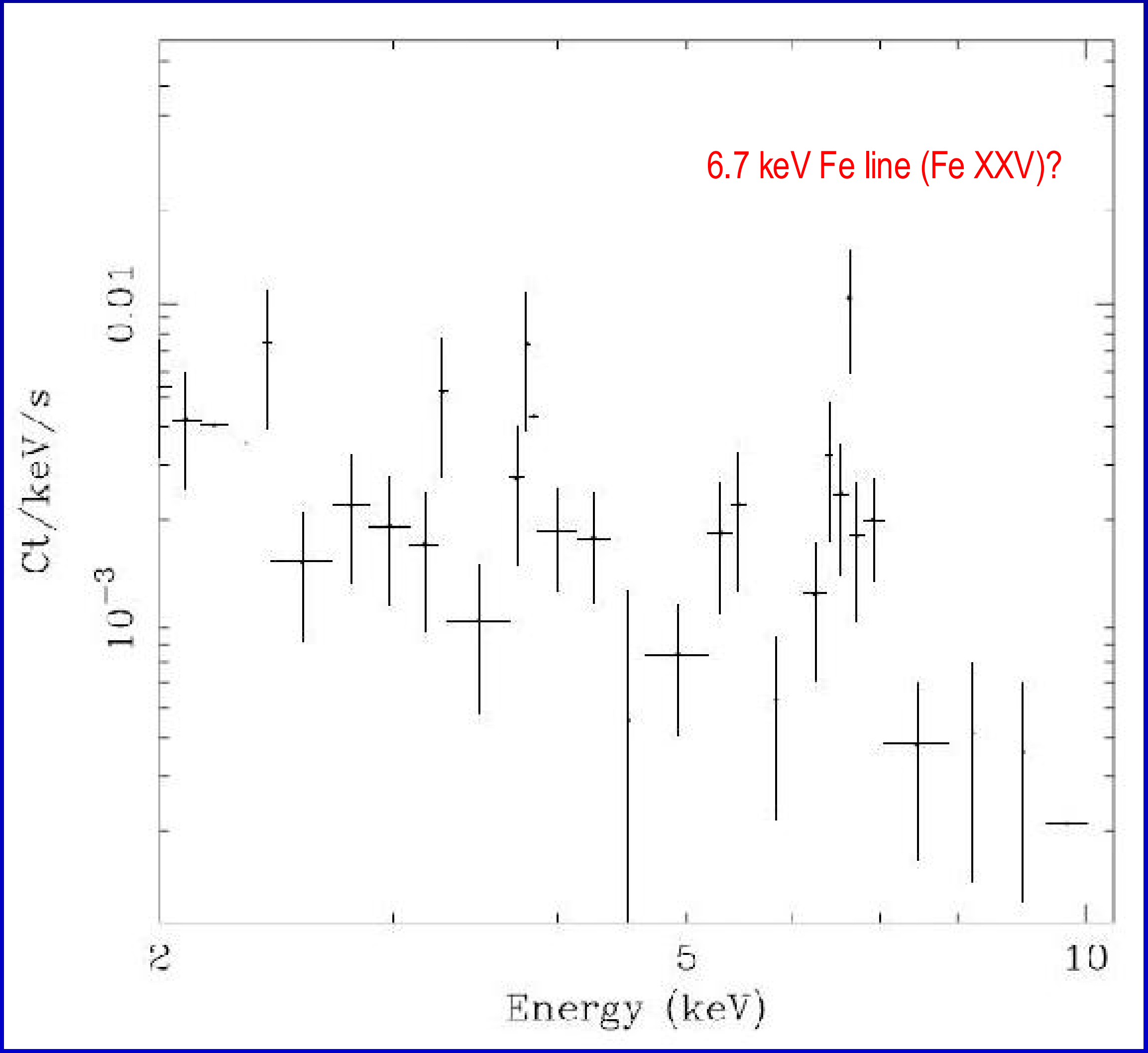

Suzaku Arp 220 XIS

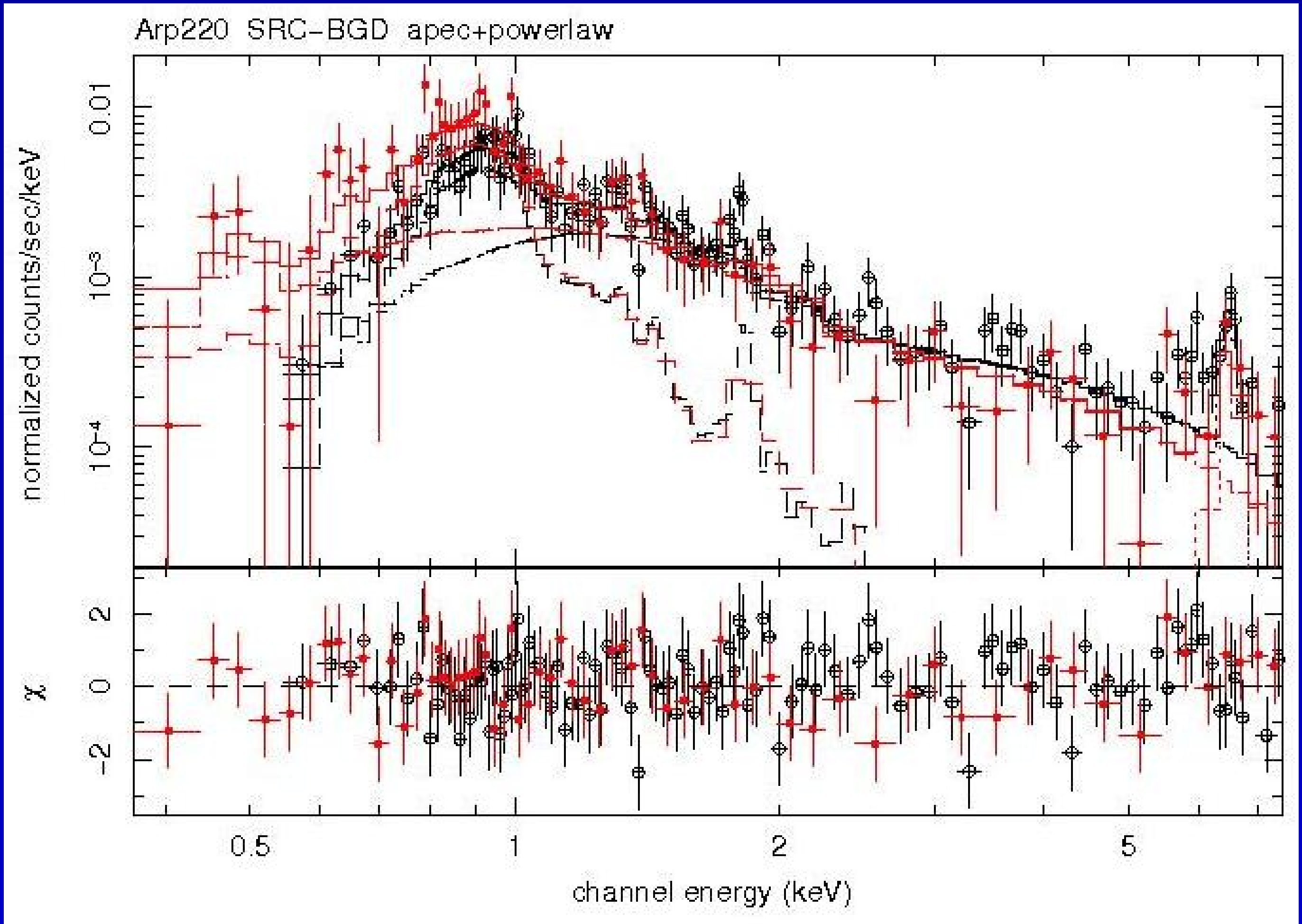

Suzaku Arp 220 XIS

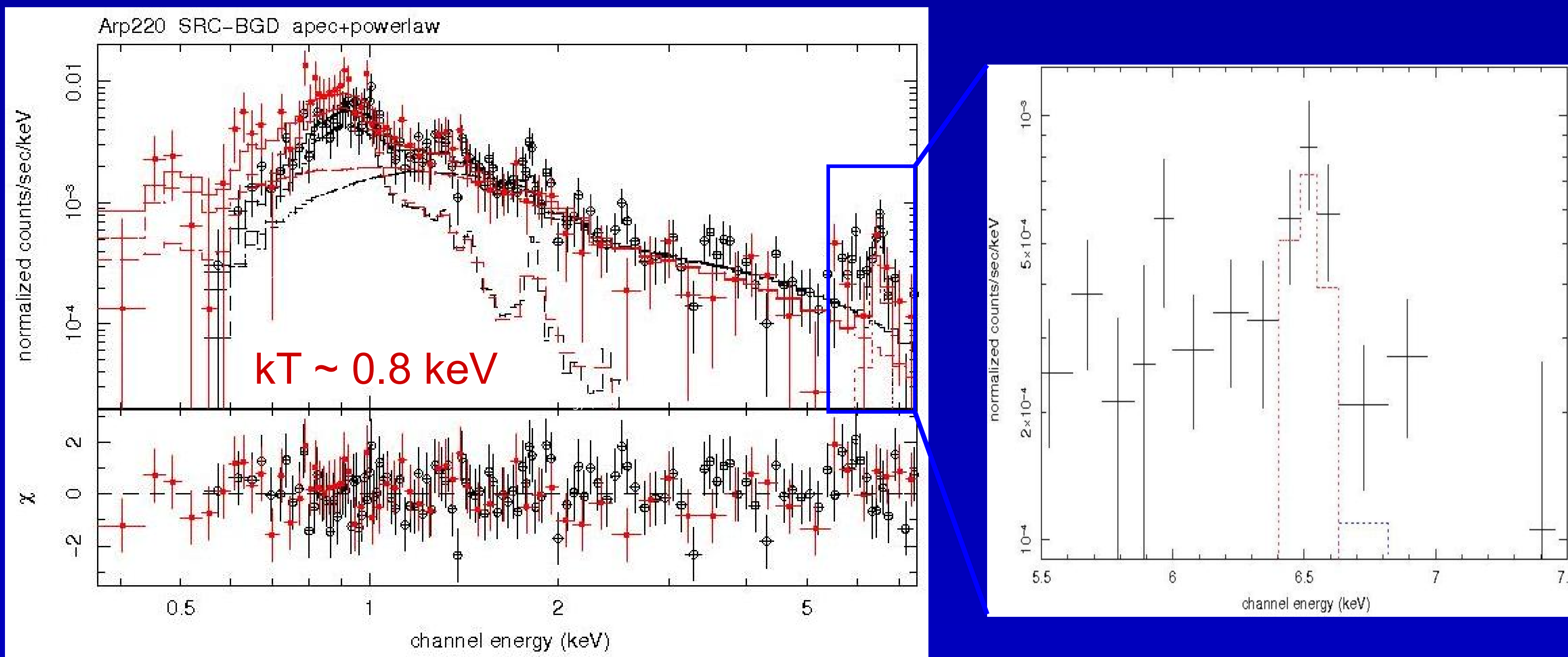

Model 1: phabs×(powerlaw+Gauss)

NH=$7.4^{+6.6}_{-3.2}\times10^{20}$ cm^{-2}

photon index $\Gamma=1.7\pm0.1$

line center=6.63 ± 0.05 keV

EW ~ 1 keV

Model 2: phabs × plasma

NH=$8.1^{+24.3}_{-7.5}\times10^{20}$ cm^{-2}

kT=$8.1^{+2.3}_{-1.7}$ keV

Abundance=2.4 ± 1.1

EM~6×10^{63} cm^{-3}

Neutral Fe-K
EW < 0.24 keV

Suzaku PIN spectrum of Arp 220

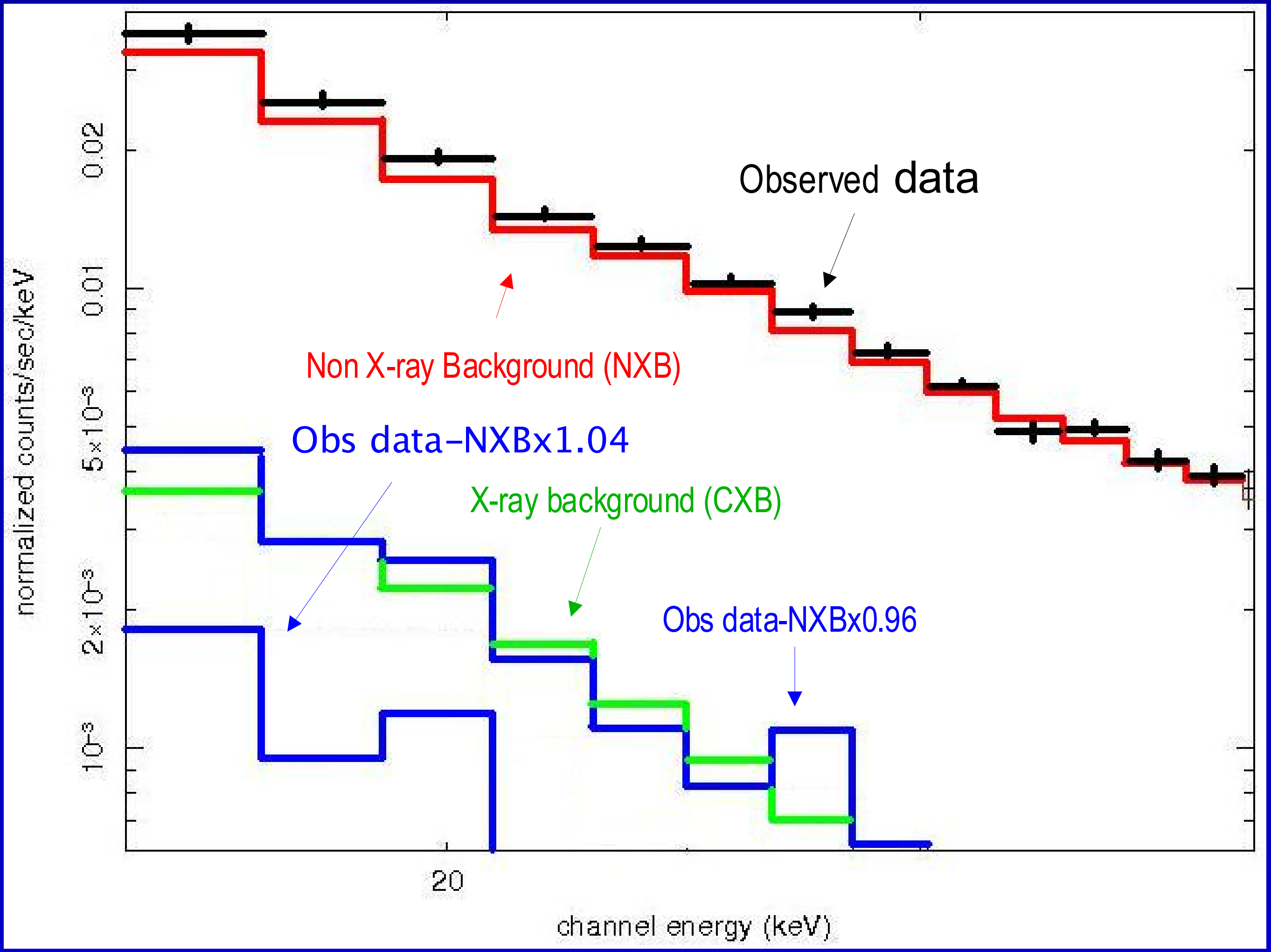

Suzaku PIN spectrum of Arp 220

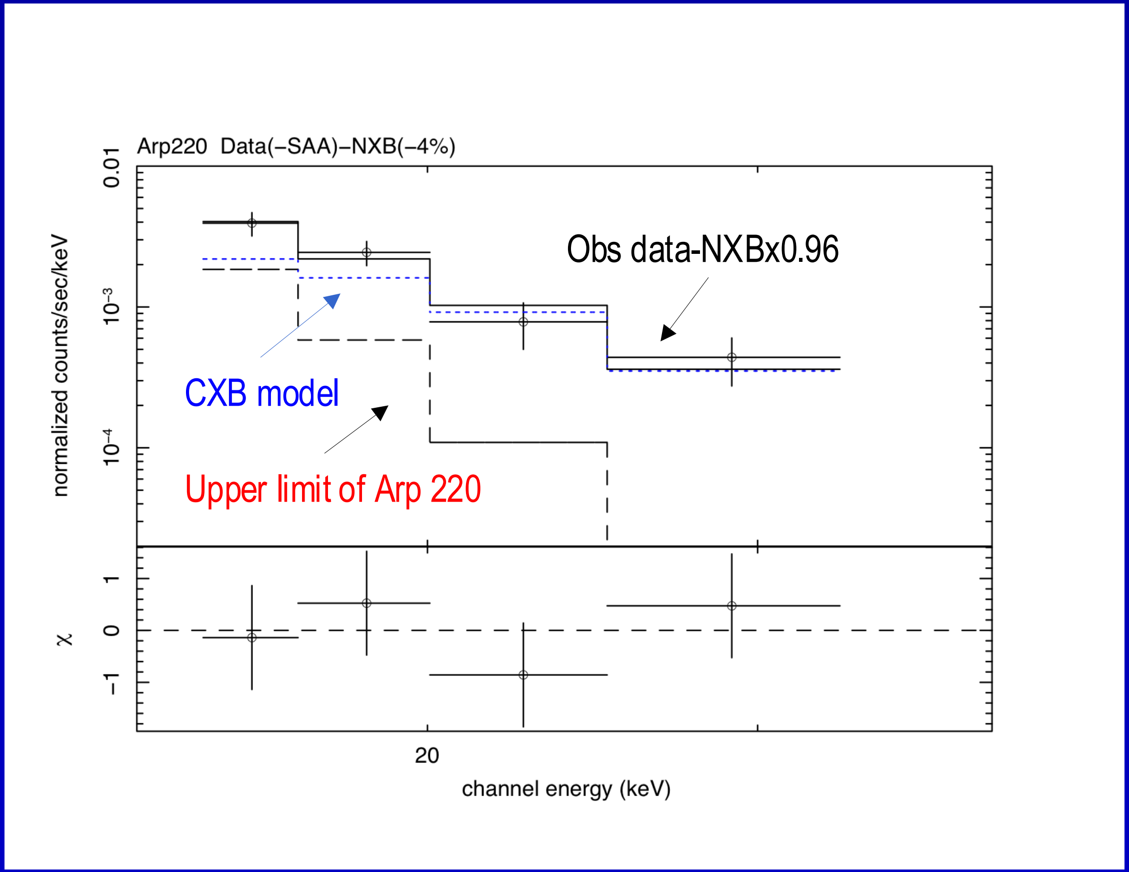

$F_{13\text{-}50\ keV} < 3.9 \times 10^{-12}$ erg cm^{-2} s^{-1}

$L_{13\text{-}50\ keV} < 2.8 \times 10^{42}$ erg s^{-1}

L_X / N_H Constraints for Arp 220

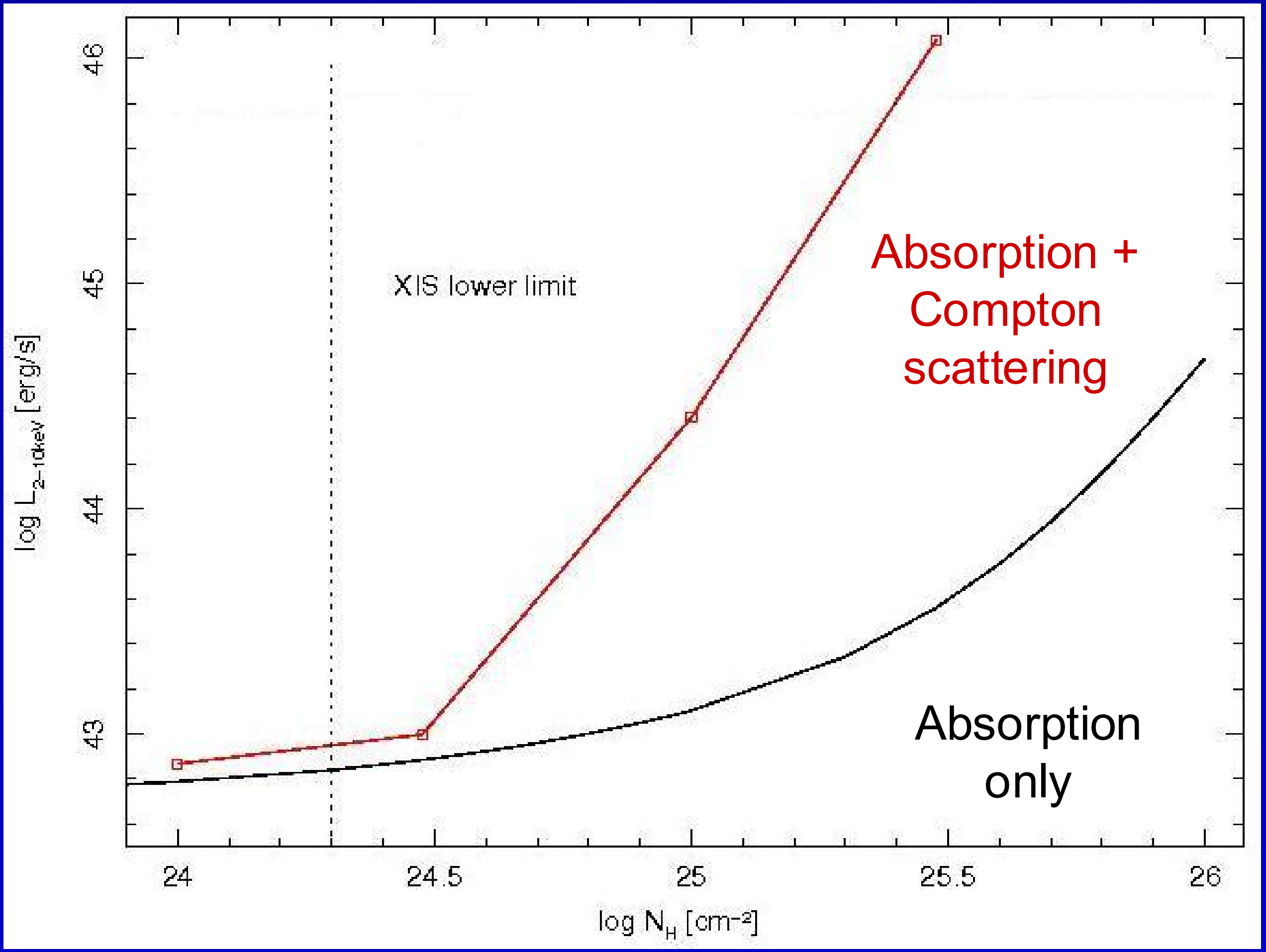

XMM Spectrum of the Superantennae

Strong reflected continuum plus a scattered power law, Fe line at E~6.4 keV (EW~1 keV).
Observed L(2-10 keV)= 3×10^{42} erg/s
(Braito et al. 03)

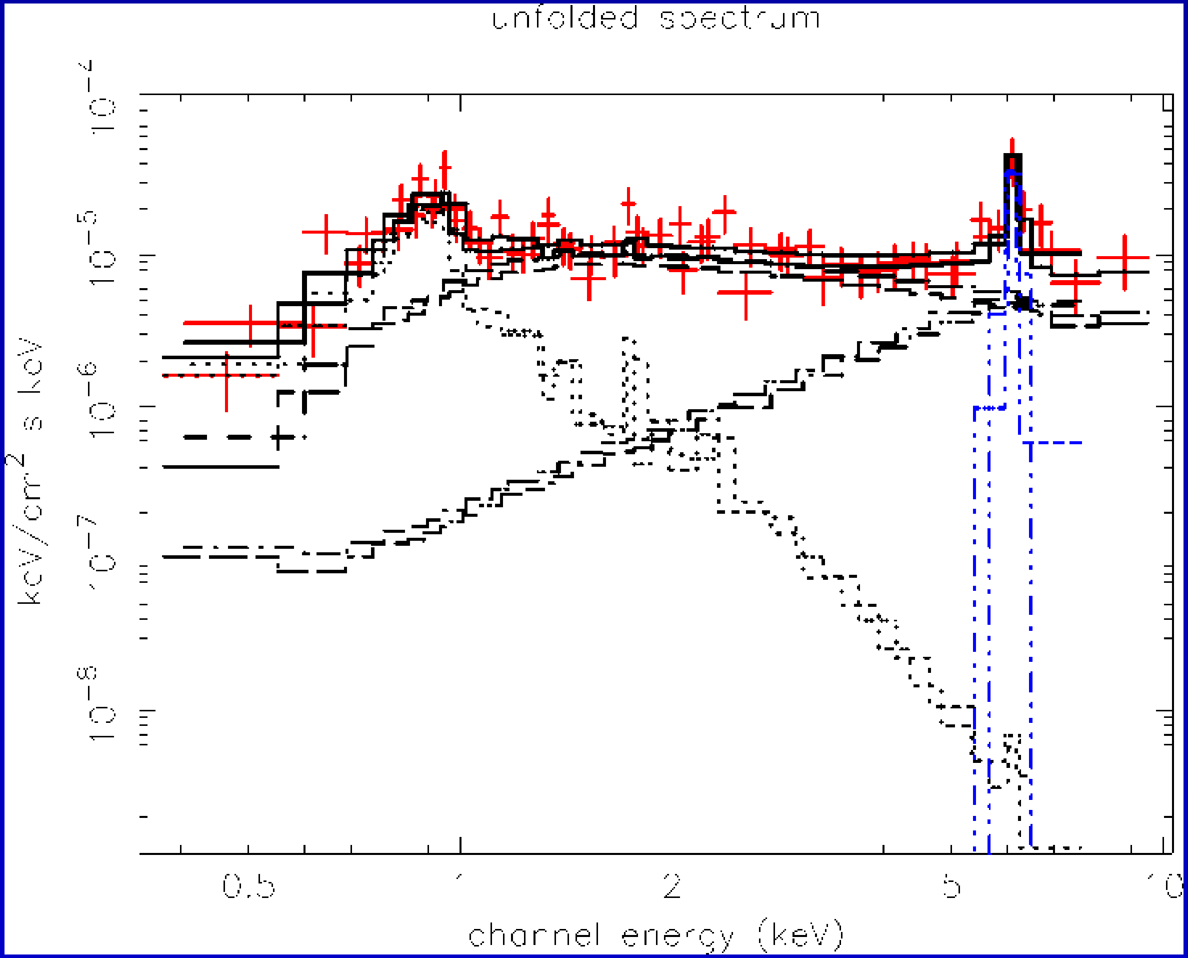

Suzaku Observation of the Superantennae

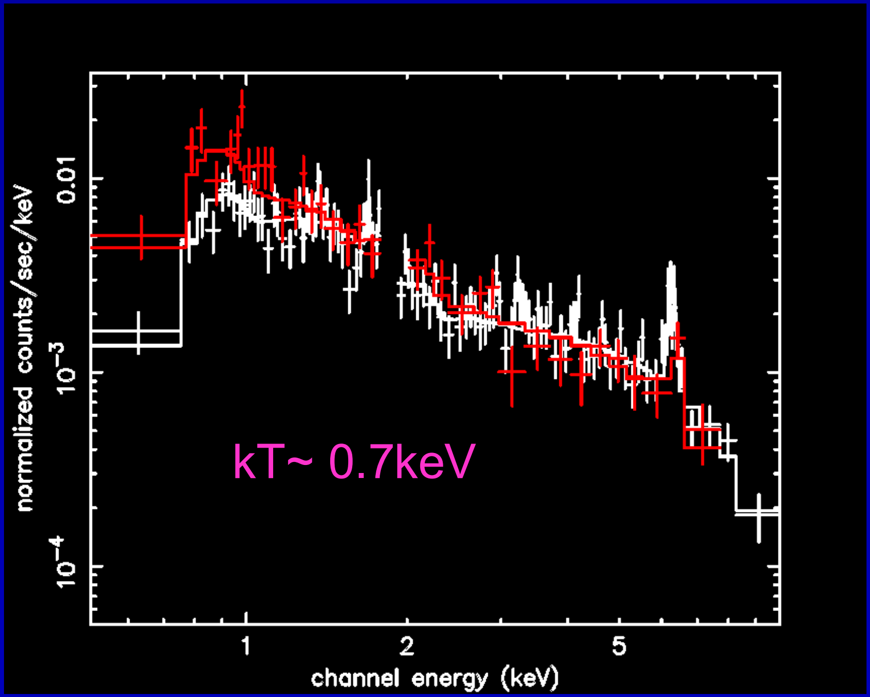

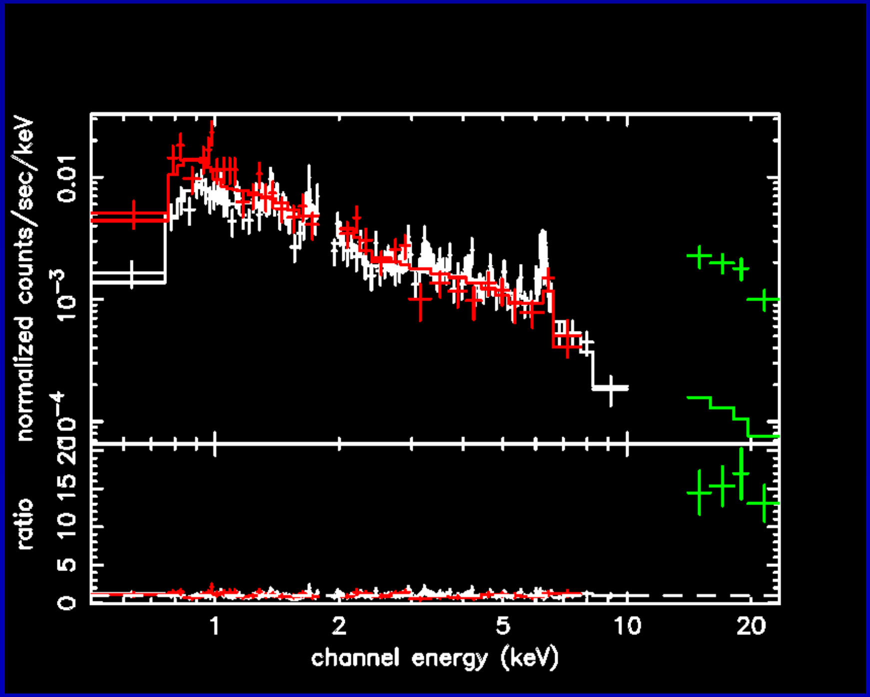

F(15-30 keV)~6 x 10^{-12} erg cm^{-2} s^{-1}

Braito et al. in prep

Suzaku FOV

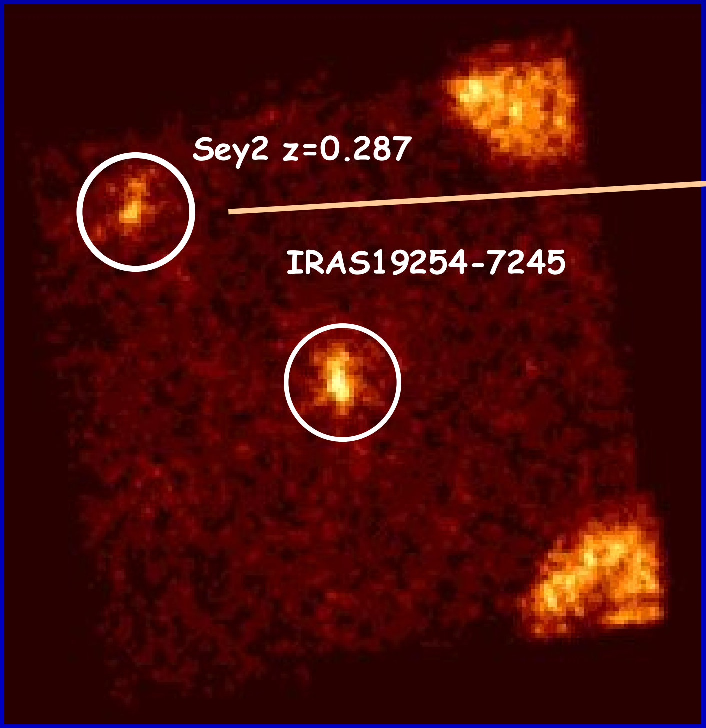
Sey2 z=0.287
IRAS19254-7245

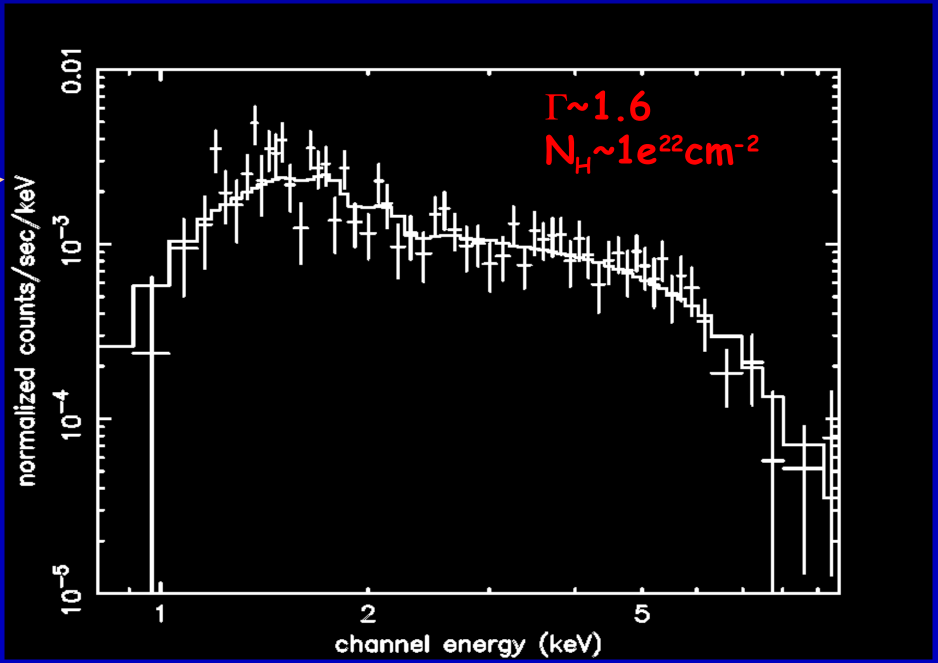
Γ~1.6
N_H~1e22cm-2
normalized counts/sec/keV
0.01
10^-3
10^-4
10^-5
1
2
5
channel energy (keV)

Superantennae Fe-K Line

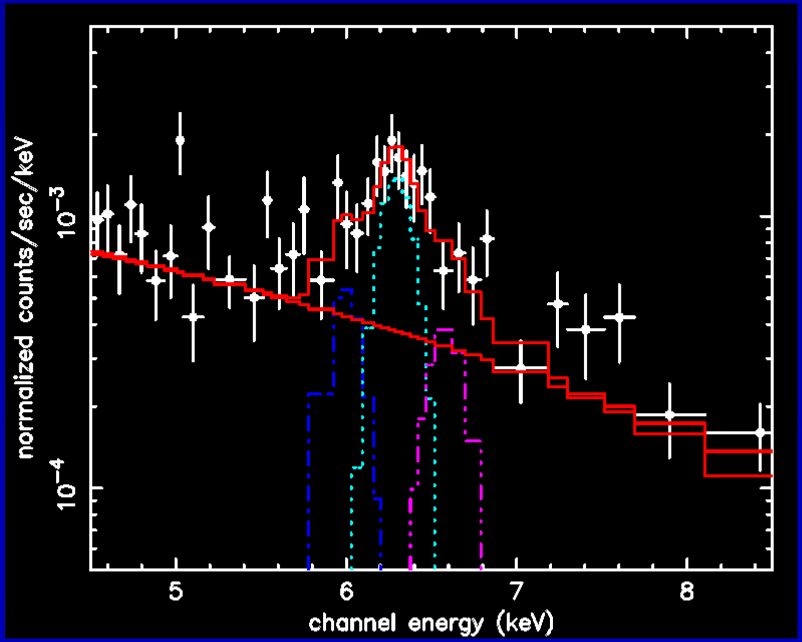

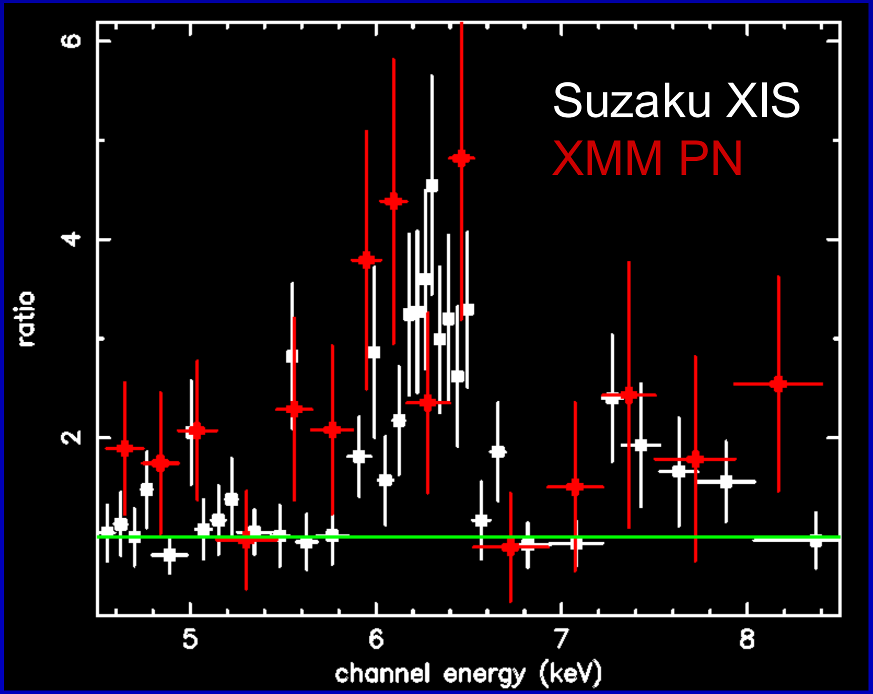

E~6.36 keV; EW~350eV
E~6.68 keV; EW~800 eV
E~6.99 keV; EW~300 eV

Broadband Fits

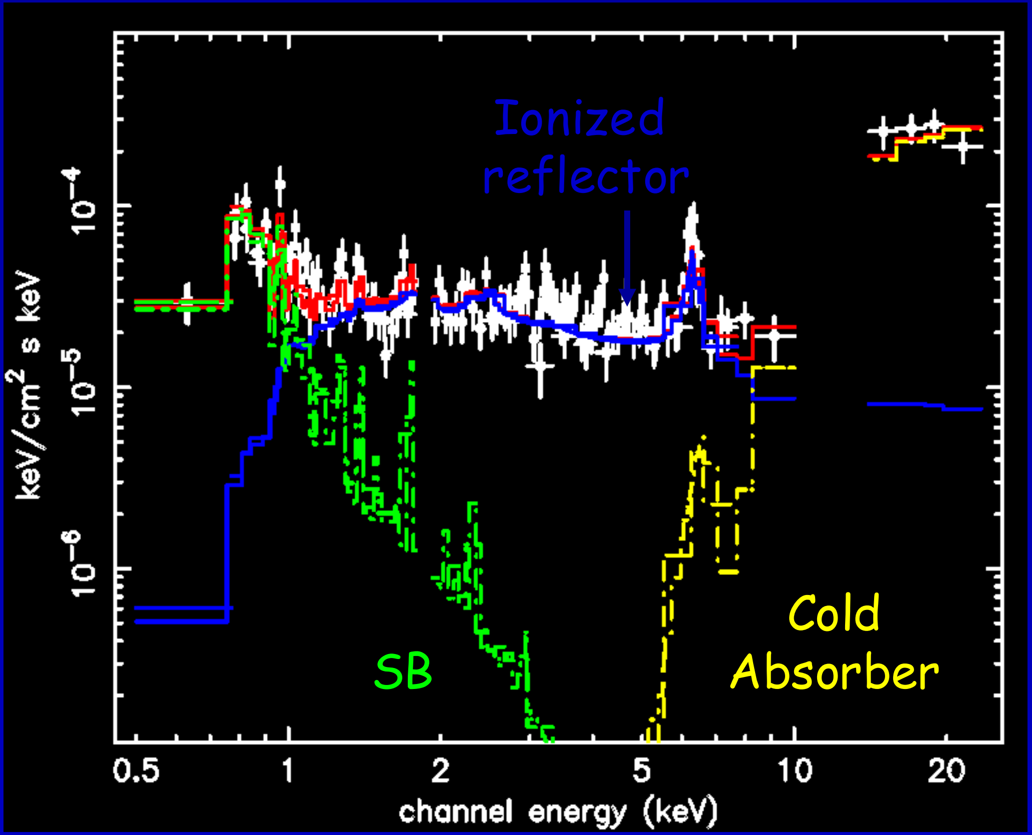

ξ~1000 erg cm s^{-1}
N_{H1}~10^{22}cm^{-2}
N_{H2}>2x10^{24}cm^{-2}
L (2-10 keV)~10^{44} erg/s

High kT plasma fit: kT~7 keV Z~2.5Z_{SUN} and $L_{2\text{-}10keV}$~10^{42} ergs s^{-1}

Other Suzaku Data / XAssist

- XAssist (http://www.xassist.org) now can reduce XIS data similar to how XMM and Chandra data are handled, follows ABC guide
  - Source detection uses SExtractor with Mexican-Hat filter but needs tuning for bright sources
  - Currently does not reprocess XIS data but will be added soon
- Script being developed to process PIN data (also follows ABC guide steps)

Mrk 273

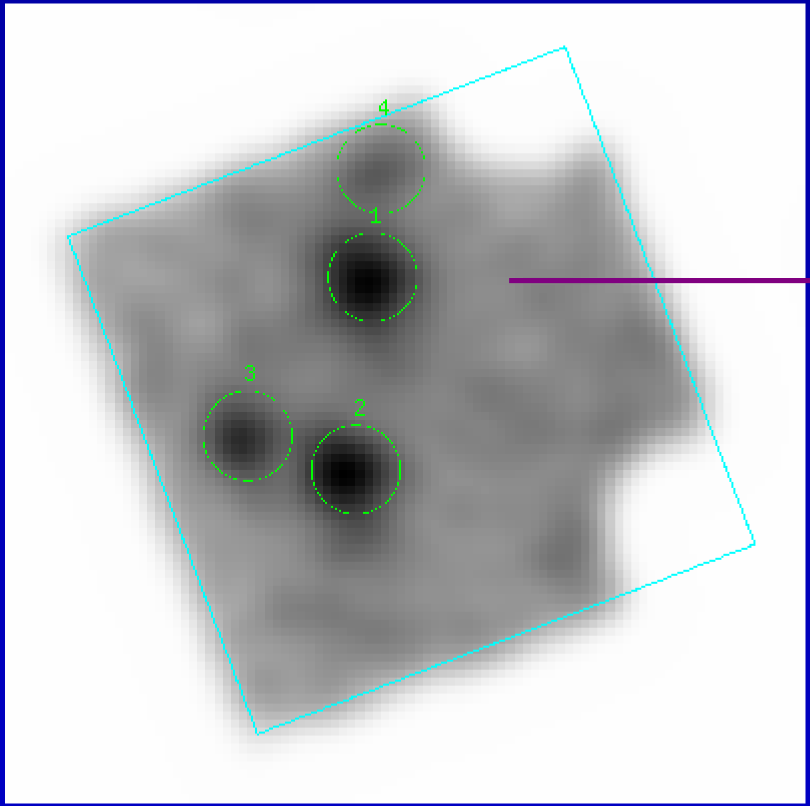

1
2
3
4

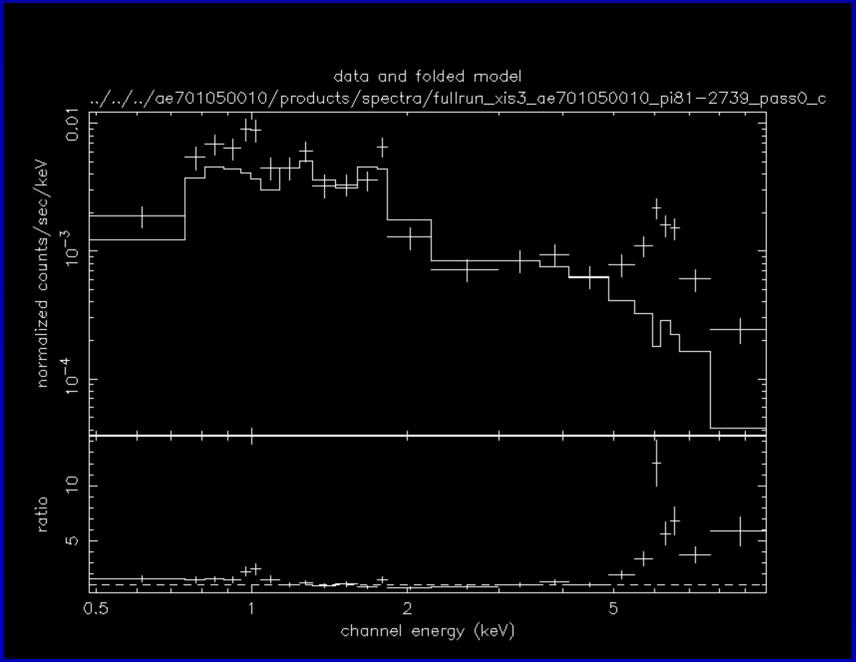

data and folded model
../../../ae701050010/products/spectra/fullrun_xis3_ae701050010_pi81-2739_pass0_c
normalized counts/sec/keV
ratio
channel energy (keV)

IRAS 08572+3915

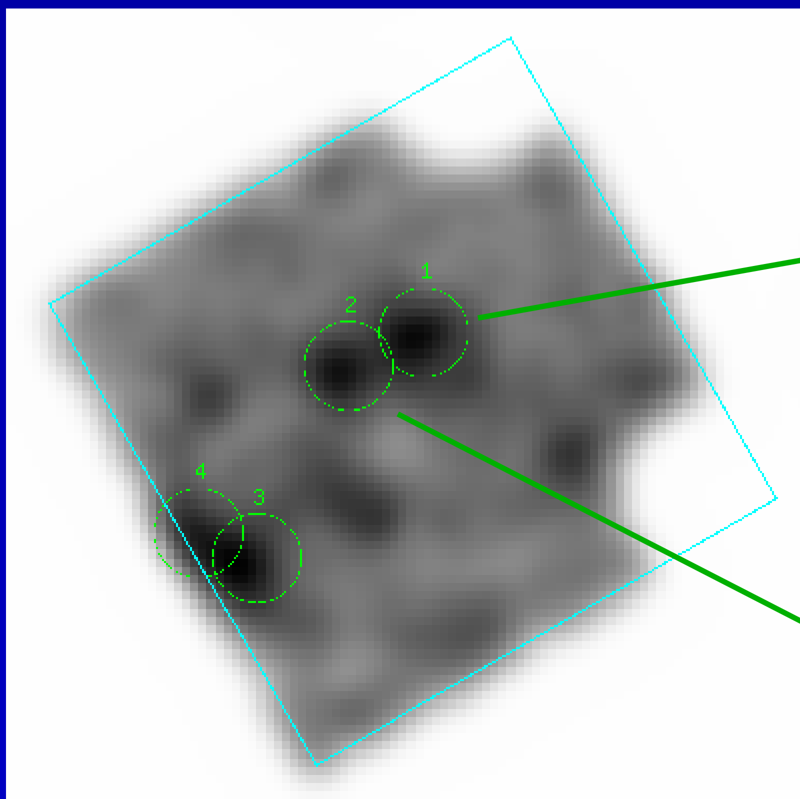

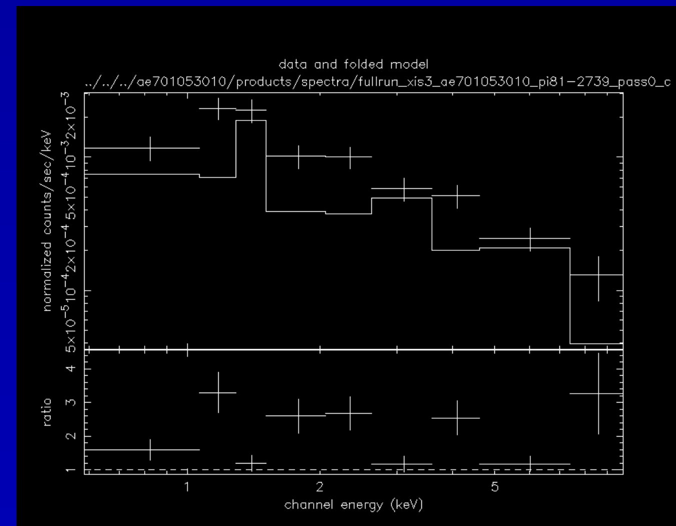

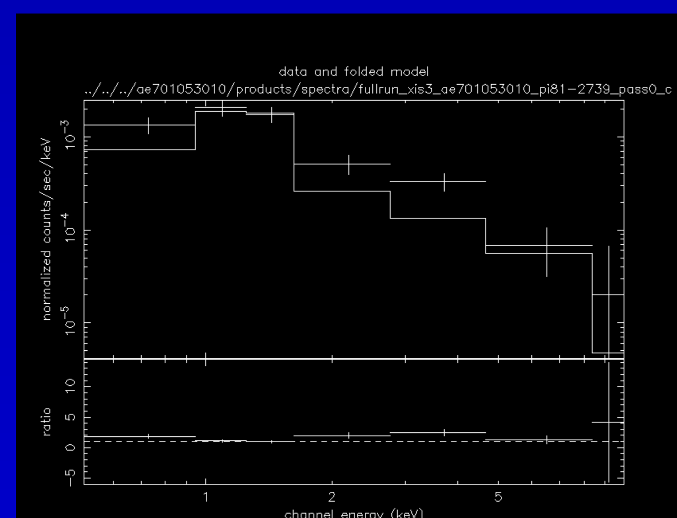

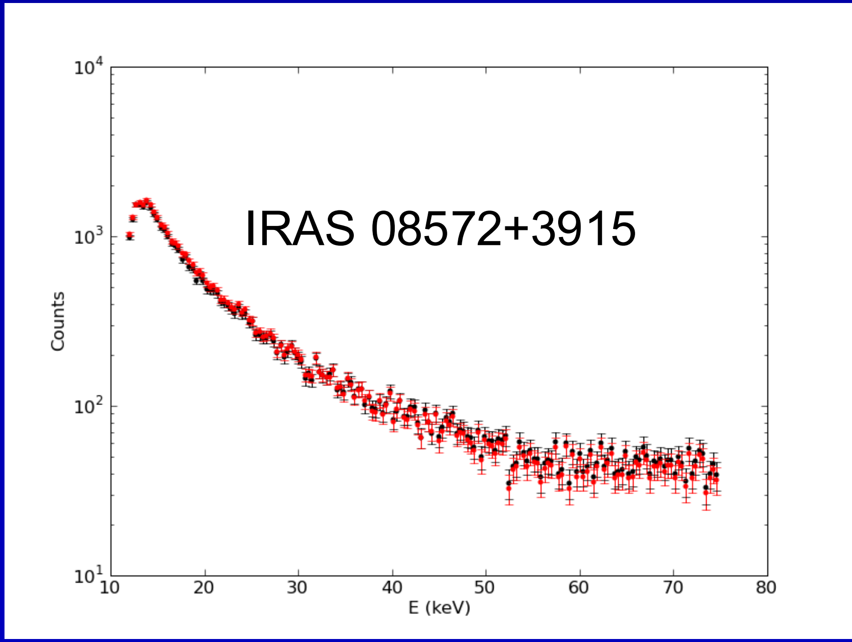

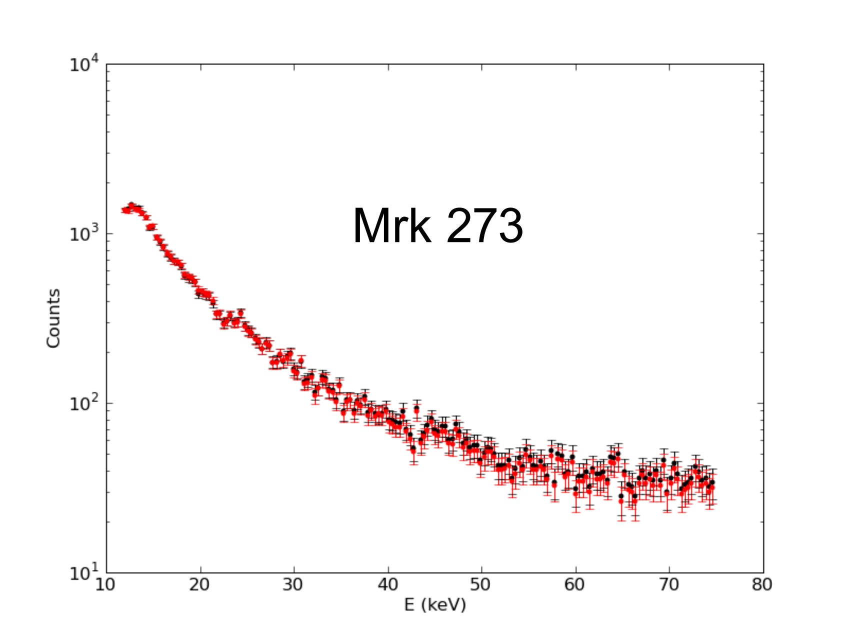

Source
NXB + CXB

Appropriate backgrounds and responses downloaded automatically

Conclusions

- Fe-K line confirmed in Arp 220 (XMM ~ 3σ, Suzaku ~ 8σ), shown to be ionized
- Hard X-ray emission above 10 keV detected for first time in the Superantennae, Fe-K emission is probably complex
- Many ULIRGs too faint and/or have nuclei too complex (e.g., NGC 6240) for HXD, need imaging v. hard X-ray observations to detangle AGN